lajss.org
Latin American Journal of Solids and Structures
www.lajss.org

Impact of parameters on damage indicators of structures: Symbolic data analysis and principal components

Rebeca Vasconcelos[a*], Graciela Doz[b], José Luís Vital de Brito[c]

[a] Federal Institute of Tocantins, Campus Palmas, Palmas, TO CEP 77020-450, Brazil. Email: rebeca.vasconcelos@ifto.edu.br
[b] University of Brasilia, Campus Darcy Ribeiro, Brasilia, DF CEP 70910-900, Brazil. Email: graciela@unb.br
[c] University of Brasilia, Campus Darcy Ribeiro, Brasilia, DF CEP 70910-900, Brazil. Email: jlbrito@unb.br

* Corresponding author

Abstract

A number of techniques have been proposed for the detection of damage to structures. Some of these techniques are based on vibrational data, whereby changes in physical properties can be identified through alterations in vibrational characteristics. The majority of techniques are based on variations of modal parameters. The direct utilization of accelerations offers considerable advantages in damage detection, making the process more rapid and more straightforward by eliminating the necessity for an identification stage. The paucity of research into raw dynamic data (accelerations) can be attributed to the considerable volume of data that must be stored and manipulated. Some authors suggest Symbolic Data Analysis (SDA) and Principal Components Analysis (PCA) as techniques for reducing the volume of data without compromising its fundamental characteristics. The objective of this study is to examine the number of categories utilized in SDA and the number of principal components in PCA that yielded the optimal damage state classification results when applied to experimental data from a simply supported beam and numerical data from a four-story Benchmark. Two techniques for determining the number of SDA categories are put forth for consideration.

Keywords

Structural damage identification, symbolic data analysis, principal component analysis, clustering, Sturges' rule.

Graphical Abstract

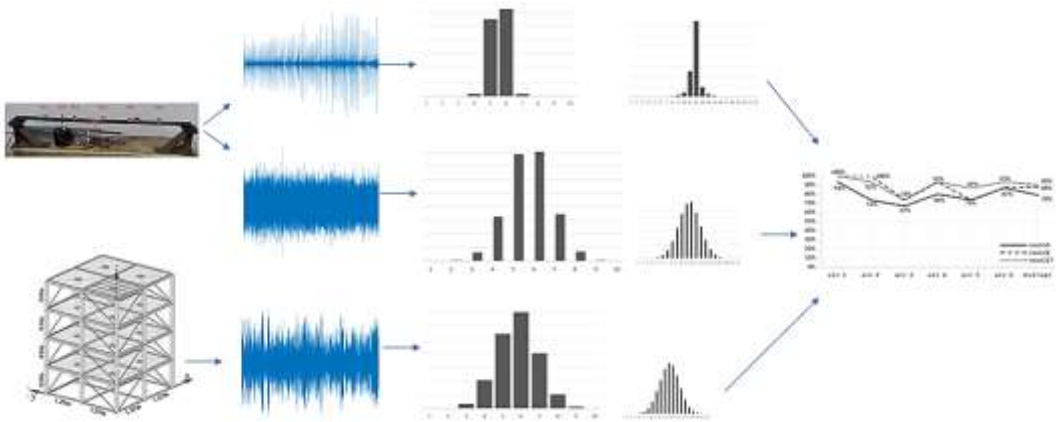

1 INTRODUCTION

In recent decades, there has been a notable increase in investment aimed at identifying damage, with a particular focus on historical and/or large-scale structures. Such structures, in the majority of cases, have a service life that exceeds the design life, a high replacement cost, a high historical, social, and economic value added, and are prone to cause greater harm to users in case of collapse. Consequently, justifying greater investments in damage investigations, repairs and maintenance.

It is inevitable that deterioration will occur due to environmental exposure, destructive excitation forces and structural use (Farrar e Worden, 1975). Civil structures may sustain damage as a result of extreme events or accumulate damage over time due to a number of factors (Nozari et al., 2017). In normal or excessive loading conditions (Sanayei et al., 2015), as a consequence of environmental, operational and/or human-induced influences, these structures become vulnerable to a range of damage types, including degradation, deterioration, corrosion, creep, fatigue, shrinkage, erosion, etc. It is therefore crucial to implement effective predictive maintenance strategies, encompassing the monitoring of structures with the objective of extending their life cycle, maintaining their functionality, preventing catastrophic events, ensuring safety, and protecting human lives. Additionally, such strategies should facilitate the early identification of damage, thereby, reducing the costs associated with subsequent repairs. (Ren e Peng, 2005; Dackermann et al., 2014; Abdeljaber et al., 2017; Dackermann et al., 2018).

Visual or localized experimental methods, such as visual inspections, acoustic or ultrasonic methods, magnetic field methods, radiography, and thermal field methods, are generally less costly but do not quantify structural performance. Furthermore, these methods require that the vicinity of the damage be inspected and accessible, which is not always the case in complex and/or large structures, as evidenced by the collapse of the Hintze Ribeiro Bridge in Portugal, which occurred despite undergoing periodic visual inspections, not having any major repairs being requested (Branco, 2013).

The necessity for quantitative methodologies for global damage detection applicable to complex structures has driven the development and ongoing research of tools that identify damage through non-destructive testing (NDT). The concept of Structural health monitoring (SHM) was developed to ensure the safety and reliability of engineering structures, taking into account different perception levels (Delo et al., 2024). By extracting, processing, and monitoring features related to their mechanical behavior, SHM provides a diagnosis of the state of the material, structural elements, and the structure as a whole (Amaral, 2022).

It is established that modal parameters, including natural frequencies, damping ratios, and structural vibration modes are functions of a structure's physical properties, specifically mass, damping, and stiffness. Accordingly, they are of paramount importance in the context of structural health monitoring (SHM), as alterations in physical properties can be discerned through modifications in vibrational characteristics, thus enabling an evaluation of the structure's present condition (Pandey e Biswas, 1994; Mazzeo et al., 2024).

Vibration analysis offers significant benefits across a wide spectrum of engineering fields, as evidenced by the research of Bourdalos et al., 2024. This includes the assessment of wind turbines (Weijtjens et al., 2024; Drangsfeldt and Avendaño-Valência, 2024), aircrafts (Hickman et al., 1991), transmission towers (Bel-Hadj et al., 2024); 3D prints (Wojtczak et al., 2024), bolts (Rashid, et al., 2024), bridges (Tomassini et al., 2024; Dederichs e Oiseth, 2024), vaults (Sabbà et al, 2024; Bru et al., 2024), masonries (Latha e Ray-Chaudhuri, 2024), among others. Vibration-based Structural Health Monitoring (SHM) employs a diverse range of novelty detection approaches, including methods inspired by intelligent design and drawing parallels to structures found in nature. These inlcude the natural defenses of the human body at the cellular level (Delo et al., 2024) and spider webs (Masmeijer et al.,2024).

SHM methods are grouped according to a number of criteria, whether the method is model-based or non-model-based methods, linear or nonlinear methods, continuous monitoring methods or those applied to damage detection from extreme events, etc.

According to Rytter (1993), for demage detection, the methods can be classified into four levels, with the higher the level, the greater the knowledge of the damage and, consequently, the greater the complexity of the method. These levels are as follows: level 1 is the detection of the damage, level 2 is the location of the damage, level 3 is the quantification of the damage, and level 4 is the prediction of the residual life of the structure.

In the opinion of Doebling et al. (1998), structural damage identification methods can be separated into two large groups: those based on vibrational data and those based on models. Model-based methods employ with techniques that facilitate reaching level 3 on the Rytter scale. However, they are associated with several drawbacks, including a high computational cost, the necessity for reliable numerical models of complex structures, and the need for model updates. This can result in the concealment of minor damage-related changes due to errors inherent to the mode (Friswell, 2007).

Vibration-based methods offer the distinct advantage of not necessitating the creation of a numerical model of the structure to be monitored. When unsupervised (i.e., without the need for pre-identification of the recorded signals), they

achieve levels 1 and 2 on the Rytter scale, and when supervised (i.e., requiring information about the data to be used), they can reach up to level 3. The prediction of level 4 is typically associated with the fields of fracture mechanics, fatigue life analysis, or structural design evaluation.

Supervised methods include those that use machine learning to detect damage to structures. These can be divided into data-based methods and physics-based methods (Yuan et al., 2024). They are trained with large amounts of data or physical laws and principles to identify complex patterns, with the goal of "learning" to recognize unique characteristics of a structure and, by comparison, identify deviations that indicate the presence of damage.

Several data-driven machine learning methods, such as Convolution Neural Network (Duan et al., 2019; Teng et al., 2019; Jesus et al., 2020; Lu et al., 2024), Transfer Learning (Yuvaraj et al., 2020; Chen et al., 2021), Long Short-Term Memory (Sony et al., 2022), Bayesian Model (Wang et al., 2020; Zhang et al., 2022), Enconder-decoder (Bang et al., 2019), Artificial Neural Network (Chaim et al., 2018), Deep Learning (Rojas et al., 2019; Avci et al., 2021), and physics-based (Fan et al., 2021; Vadyala et al., 2022) have been successfully applied to detect cracks and damage in beams, roads, railroads and bridges.

However, methods based on machine learning have the disadvantage of requiring a large number of examples to train the algorithm, which are not always available, as well as the high computational cost of the various training sessions that the algorithm must undergo (Haykin, 1999).

Doebling et al. (1998) present a comprehensive literature review of vibration-based damage identification methods, which analyze changes in basic modal properties (natural frequencies, vibration modes and their curvatures, stiffness matrices and flexibility matrices) and which analyze structural changes in model parameters.

The literature review reveals that most structural damage detection techniques are based on variations in modal parameters or indicators derived from them. One limitation of this approach is the impossibility of directly using dynamic responses. Many structural health monitoring systems include different types of response sensors that measure, for example, accelerations, velocities, displacements, or deformations. (Kullaa, 2024). The direct use of accelerations offers significant advantages in damage detection, as it makes the process faster, simpler, and more direct, eliminating the need for a modal identification stage (Farrar and Worden, 2012). It is possible to develop an automatic structural integrity monitoring system capable of detecting structural changes in real time, using only the raw acceleration signals from the structure (Soares, 2022).

The limited exploration of in-situ measurements arises from the fact that dynamic measurements lead to the storage and handling of large volumes of data, as they are often monitored by multiple measurement channels. Thus, it is necessary to employ techniques that allow raw data to be used in a practical and relevant way, such as in the case of adapted representations known as "symbolic data," which enable the manipulation of large databases by compressing them without losing the generality of the original information (Cury et al., 2010; Crémona et al., 2011; Cury and Crémona, 2012; Cury et al, 2012; Cardoso et al., 2019a; Cardoso et al., 2019b).

One of the primary challenges in employing raw acceleration data lies in efficient data compression without compromising the preservation of crucial information. The selection of appropriate data windows, parameters, and compression techniques (damage indicators) is essential to prevent the loss of information relevant to the analysis and detection of structural damage. (Cury, 2010).

Alves (2016) assessed a collection of damage indicators (Symbolic Data Analysis, Principal Component Analysis, Frequency Response Function, Fourier Transforms, Spectral Density, Wavelets, and High-Order Statistical Parameters) derived from acceleration data, coupled with various classification methods for structural change detection.

The aim of this paper is to investigate the impact of parameter choices employed in damage indicators on the detection of distinct structural states. Among the various parameters, the number of categories in the histogram for transforming raw data into symbolic data and the number of components in principal component analysis were discussed. The study was applied to experimental data from a laboratory-tested simply supported beam subjected to impact and random vibration excitations, analyzed by Alves (2016), and to numerical data from a finite element simulation of a 4-story Benchmark proposed by Johnson et al. (2002) as a standard structure for testing damage detection methods. The proposed methodology is based on an unsupervised method for structural state detection through the analysis of damage indicators derived from structural accelerations using the k-means clustering technique with sample initialization and the cityblock similarity metric.

2 THEORY

2.1 Damage Indicators

Damage indicators in civil engineering structures are observable measures or characteristics that provide information about the structural condition of an infrastructure. These indicators may include visible signs of deterioration, such as cracks, deformations, corrosion, or may be quantitative, such as displacements, vibrations, or loss of endurance (Cury et al., 2014).

The purpose of damage indicators is to provide an understanding of structural integrity, assisting in the early identification of potential problems and the implementation of appropriate maintenance or repair measures to ensure the safety and durability of structures.

The following presents two damage indicators applied to the analysis of dynamic acceleration signals.

2.1.1 Symbolic Data Analysis (SDA)

Symbolic data analysis manipulates data concepts, enabling them to be represented in a more compact manner while preserving the same richness of information. They are called symbolic because they express the inherent internal variation of each variable, considering the specificities of the database.

Figure 1 presents the classical signal from a sensor (on the left) and the symbolic representation of the signal (on the right) in a histogram.

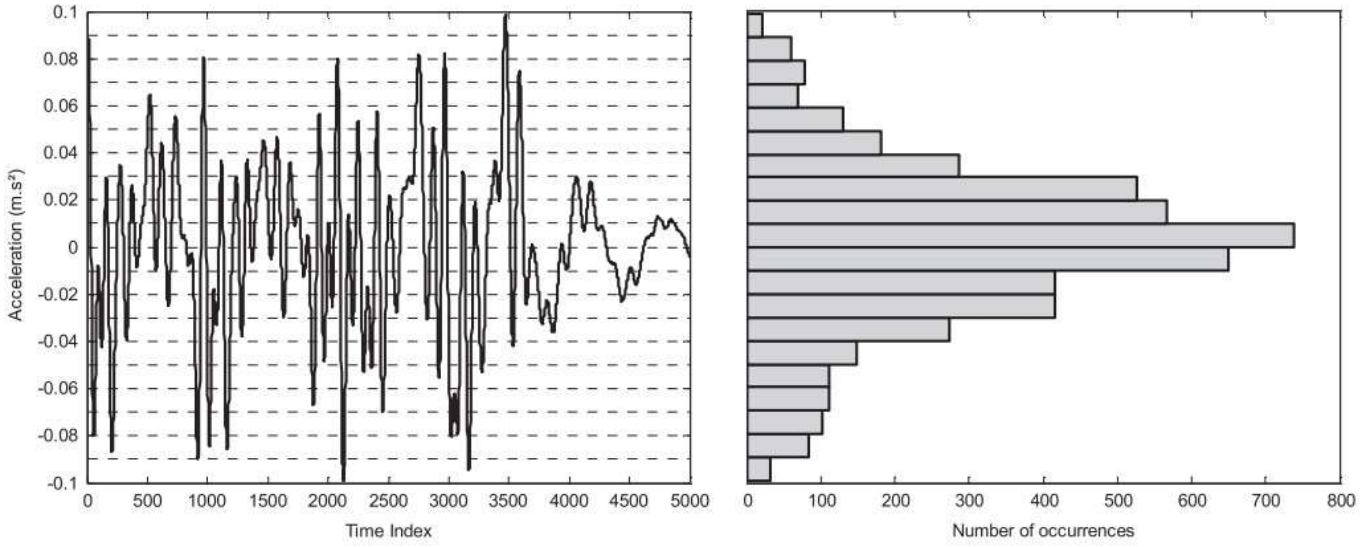

Figure 1 Example of transforming accelerations (classical data) into symbolic data.

The following presents an example of a symbolic data set containing three dynamic tests described by histograms $\Omega = \{E_1, E_2, \dots, E_n\}$

$$\begin{aligned} E_1 &= \{[0-20](0{,}20); [20-40](0{,}25); [40-60](0{,}25); [60-80](0{,}30)\} \\ E_2 &= \{[0-20](0{,}05); [20-40](0{,}30); [40-60](0{,}40); [60-80](0{,}25)\} \\ E_3 &= \{[0-20](0{,}10); [20-40](0{,}15); [40-60](0{,}60); [60-80](0{,}15)\} \end{aligned} \quad (1)$$

with the intervals adopted within the square brackets, and the percentage of incidence per test in parentheses. In this case, we say that four categories were used, since four intervals were considered in the data division.

2.1.2 Principal Components Analysis (PCA)

Principal component analysis (PCA) is a multivariate statistical technique, also known as Karhunen-Loève transform or orthogonal decomposition (Figure 2), which aims to reduce the dimensionality of datasets while keeping only the "main" information. In this way, the dataset undergoes mathematical modifications to highlight its similarities and differences.

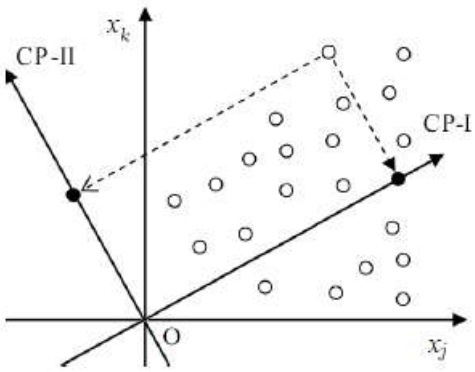

Figure 2 Hypothetical example of a 2D transformation into principal components.

In the applied case, its approach aims to detect abnormal variations in the acceleration data of the analyzed structures, eliminating the effects of environmental conditions on the vibrational data, without the need for environmental variable measurements.

The method projects the original acceleration signals contained in a higher-dimensional space p, into a new set of Cartesian coordinates of lower dimension q (z_1, z_2, ..., z_q), where q<p. In this way, the new coordinates are linear combinations of the original coordinates, organized from highest to lowest variance.

By considering the acceleration vector x_k (k=1, ..., p), it is possible to construct the acceleration matrix $X \in \Re^{nxp}$, where p is the number of accelerometers to be considered and n is the number of readings. PCA therefore provides a linear projection of the data from dimensions p towards a reduced dimension q. This transformation is represented by

$$Z = X\Psi \tag{2}$$

where $Z \in \Re^{nxq}$ is the acceleration matrix with the transformed data and $\psi \in \Re^{pxq}$ is the transformation matrix. The transformation matrix ψ can be calculated from the extraction of the q eigenvectors of the covariance matrix of X, here denoted by C

$$C = \begin{bmatrix} var(x_1) & cov(x_1,x_2) & \cdots & cov(x_1,x_p) \\ cov(x_2,x_1) & var(x_2) & \cdots & cov(x_2,x_p) \\ \vdots & \vdots & \ddots & \vdots \\ cov(x_p,x_1) & cov(x_p,x_2) & \ldots & var(x_p) \end{bmatrix} \tag{3}$$

where var(.) indicates the variance and cov(.) the covariance between vectors.

First, the degree of dependence between each of the dimensions is found, taking them two by two, and indicating how the variations are linked. Zero covariances demonstrate that there is no link between the two dimensions. The covariance between the acceleration vectors x_j and x_k is given by

$$cov(x_j, x_k) = \frac{1}{n}(A^T A), com\ A = \left[x_j - \bar{x}_j.1, x_k - \bar{x}_k.1\right] \tag{4}$$

where, $\bar{x}_j$ and $\bar{x}_k$ are the mean values of the acceleration vectors x_j and x_k, respectively, and 1 denotes the unit vector.

Next, the eigenvectors and eigenvalues of the covariance matrix C, given by

$$C.\phi = \lambda.\phi \leftrightarrow (X - \lambda.I).\phi = 0 \tag{5}$$

The eigenvalue problem can be stated as: if the product of a vector ϕ and the matrix C is equal to a scalar multiple λ of ϕ, then, ϕ is an eigenvector of the matrix C and λ is the eigenvalue of C associated with the eigenvector ϕ.

As the covariance matrix increases in dimension, the difficulty of solving the eigenvalue and eigenvector problem increases. Singular Value Decomposition (SVD) is used as a solution, which allows the matrix C to be decomposed

$$C = U\Lambda V^T \tag{6}$$

where U is the orthonormal matrix, whose columns are the vectors that define the principal components in the transformation space, V is the matrix containing the vectors of the original space, and Λ is the matrix of singular values or eigenvalues.

Once the eigenvalues and eigenvectors of the covariance matrix C have been extracted, the eigenvalues are sorted according to their magnitude. The eigenvectors corresponding to these eigenvalues are the most relevant in this direction and allow the most information from the original data set to be preserved. Since each eigenvalue is a principal component, it is intuitive to use those that are most representative.

The transformation matrix Ψ is then constructed using only q eigenvectors (columns) of the matrix U. The number of principal components chosen depends greatly on the type of problem being treated, so it is important to observe the percentages of information provided by the eigenvectors. There are cases where a single component can represent the original data without significant loss of information.

The reconstructed acceleration matrix $\hat{X}$ is calculated by

$$\hat{X} = Z\Psi^T = X(\Psi\Psi^T) \tag{7}$$

2.2 Determination of the Number of Categories in SDA

Cury (2010) presents the dependence on the choice of the number of intervals (ncat) of the histogram as a disadvantage of the SDA method, which can vary depending on the application being studied, and it is up to the user to choose the most appropriate symbolic representation.

Alves (2016) uses 10 categories in his analyses to describe the data of the simply supported beam, however, the motivation for adopting such a value is not informed.

The following presents two proposed methods for determining the number of categories of the histograms in SDA.

2.2.1 Analysis of the Conservation of Statistical Properties

Verifying the maintenance of the statistical properties of the data is a crucial step in symbolic data analysis. This step ensures that the important characteristics and relationships present in the data are preserved throughout the analysis process, ensuring the reliability and quality of the results.

To this end, the suggested number of categories can be defined by the value at which the variance between the symbolic data and the original data is less than 15%.

2.2.2 Sturges' Rule

A simple and quick method for determining the ideal number of classes (intervals) to construct a frequency distribution table in descriptive statistics was proposed by Sturges (1926), and can be calculated by

$$k = 1 + \log_2(n) \tag{8}$$

where, k is the number of classes (rounded to the nearest whole number) and n is the total number of observations (size of your dataset).

2.3 Método K-means

Implicit in the definition of damage is that the concept of damage is not meaningful without a comparison between two different states of the system, one of which is assumed to represent the initial state, and often undamaged (Doebling et al., 1998). The use of data classification techniques in dynamic signals aims to group data by structural state, thus identifying the different structural states, i.e., the presence of damage.

Data classification techniques are powerful tools that allow for organizing and interpreting large volumes of information. Through sophisticated algorithms, these methods identify patterns and group data into predefined categories, facilitating analysis and decision-making (Hastie et al., 2009).

Unsupervised methods consist of grouping a set of "unknown" (unlabeled) information into several groups (clusters). This information is associated with the clusters indirectly from calculations (degree of similarity) performed by different algorithms using different aggregation criteria (Alves, 2012).

The k-means algorithm is defined as a non-hierarchical (or partitioning) classification method in which the number of clusters is considered fixed and initially defined. The basic difference between hierarchical and non-hierarchical clustering algorithms is that partitioning algorithms search for all clusters simultaneously without imposing a hierarchical notion.

This algorithm uses the concept of centroids as the aggregation criterion to represent the clusters. These centroids are calculated from the mean of all objects in the group (Fontana and Naldi, 2009).

This algorithm seeks the best division of n objects into k groups $(C^i, i = 1, \dots, k)$ minimizing the total distance, summed over all groups, between the objects in a group and its respective center (Pimentel et al, 2003).

The k-means algorithm can be described by the following steps:

1. Select the number of clusters to be formed.
2. Assign initial values for the k centroids following some initialization criterion.
3. Assign each object to the group whose centroid has the greatest similarity.
4. Recalculate the value of the centroid of each group as the mean of the current objects in the group.
5. Repeat the previous two steps until the groups stabilize, that is, the centroids move little or none relative to their previous position.

2.3.1 Centroid Initialization Criterion

Regarding the centroid initialization criterion, various methods can be used (sampling, uniform, clusters, random, etc.). However, this article will present the results obtained with the sampling initialization criterion and, in some cases, the random criterion, as they presented the best results among the previously tested criteria.

The sampling initialization criterion uses k objects from the database chosen randomly, where k is the chosen number of clusters. A restriction was established to the algorithm of not allowing repeated objects among the initial centroids.

And, in the random initialization criterion, each object is randomly assigned to k clusters. In this case, empty clusters are not allowed.

The value of k was defined as the number of test campaigns carried out on the structure, which in this case configure different damage states in each campaign, simulating readings taken on a real structure, on different dates.

2.3.2 Dissimilarity Measure

The similarity or dissimilarity between objects is evaluated by a function that estimates the distances that separate them to create the clusters (Esposito et al, 2000). The choice of a distance measure is a relevant step in the clustering method, which consists of minimizing the sum of the distances between the objects.

The results presented in this article were obtained using the cityblock metric, as it presented the best results among the previously tested metrics.

The cityblock metric is given by the equation

$$gs(E_i, E_j) = \sum_{k=1}^{n} |E_{ik} - E_{jk}| \tag{9}$$

where gs is the degree of similarity, E_i e E_j are two hypothetical tests, and n is the number of categories of the tests.

3 APPLICATIONS

3.1 Simply Supported Beam

Experimental tests of a simply supported steel beam were conducted in the structures laboratory of COPPE/Federal University of Rio de Janeiro (UFRJ) by Alves et al. (2015) and their readings were kindly provided by Professor Ney Roitman. The beam, as well as the data acquisition system, had the characteristics described in Table 1, and was instrumented with six piezoelectric accelerometers, arranged as shown in Figure 3.

Table 1 Characteristics of the steel beam and data acquisition.

Beam length	1,46 m
Beam cross-section	76,2 x 8,0 mm (rectangular)
Data acquisition system	Lynx ADS2002
Accelerometer type	Piezoelectric – PCB, 336C31
Data acquisition time per test	10 min
Sampling period	0,00025s
Sampling frequency	4000Hz

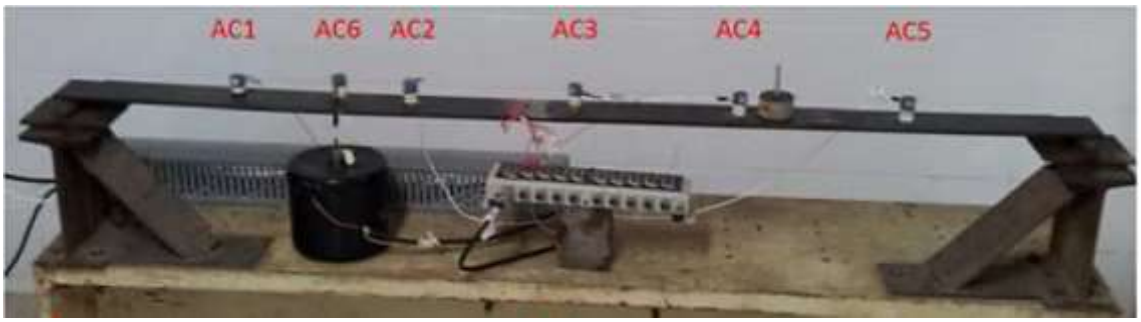

Figure 3 Simply supported and instrumented steel beam.

Tests were carried out with two types of excitations: impact tests using a hammer, impacting the beam every 10 seconds (Figure 4), and random vibration tests, using an exciter, throughout the entire test.

Figure 4 Steel beam under hammer impact, containing damage caused by a 12mm hole.

Six acquisition campaigns (six different damage states) were performed. For each campaign, three 10-minute tests were recorded. A total of 18 dynamic tests for each type of excitation, where each test had 2.4 million values obtained for each of the six instrumented sensors. A total of 259.2 million values addressed for each type of excitation.

Examples of accelerations plotted as a function of time, for each type of excitation, are contained in Figure 5.

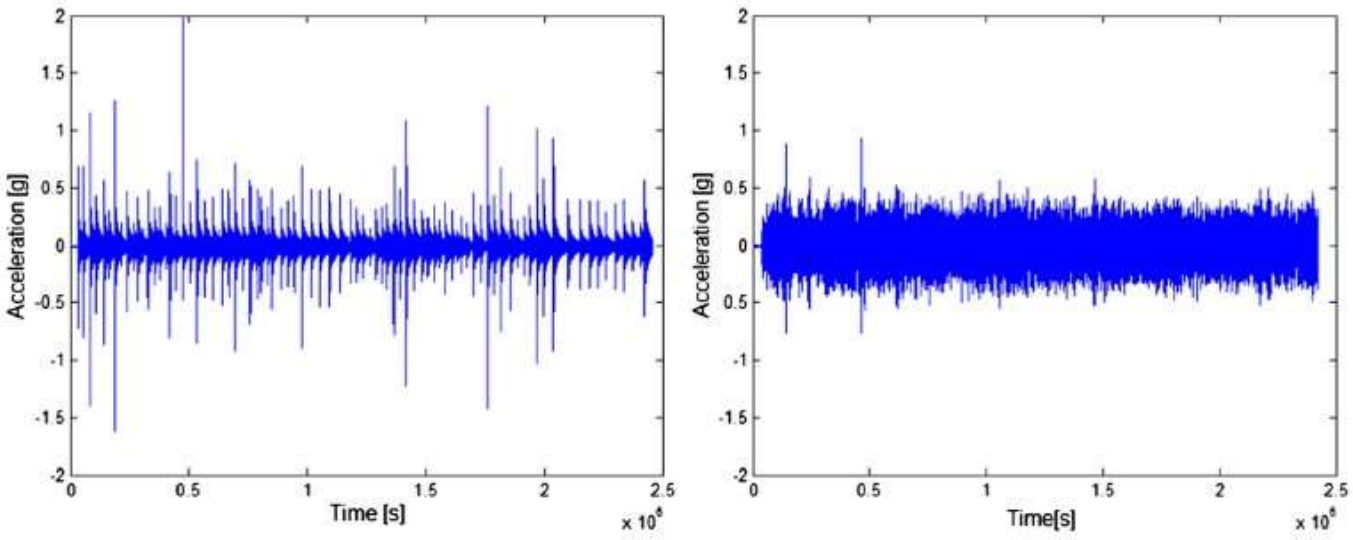

Figure 5 Examples of vibration tests performed on the beam in the laboratory: Impact (left) and random vibration (right).

Each campaign had different structural states in terms of damage, with their characteristics described in Table 2.

Table 2 Types of damage caused to the structure.

NÍVEL	DANO IMPOSTO
Intact	No damage
Level 1	Addition of a 500 g mass to 102.7 cm from the left support of the beam
Level 2	12 mm diameter round hole
Level 3	16 mm diameter round hole
Level 4	22.5 mm diameter round hole
Level 5	32 mm diameter round hole

3.2 Benchmark

The IASC-ASCE group proposed a Benchmark with the objective of establishing a standard structure for testing damage detection methods. In Phase I of the Benchmark, the working group developed a finite element analysis (FEA) code using Matlab, to simulate the dynamic response, with synthetic data, for different damage patterns of a 4-story 3D steel structure with 2x2 bays (Figure 6), built at the University of British Columbia (UBC), Canada.

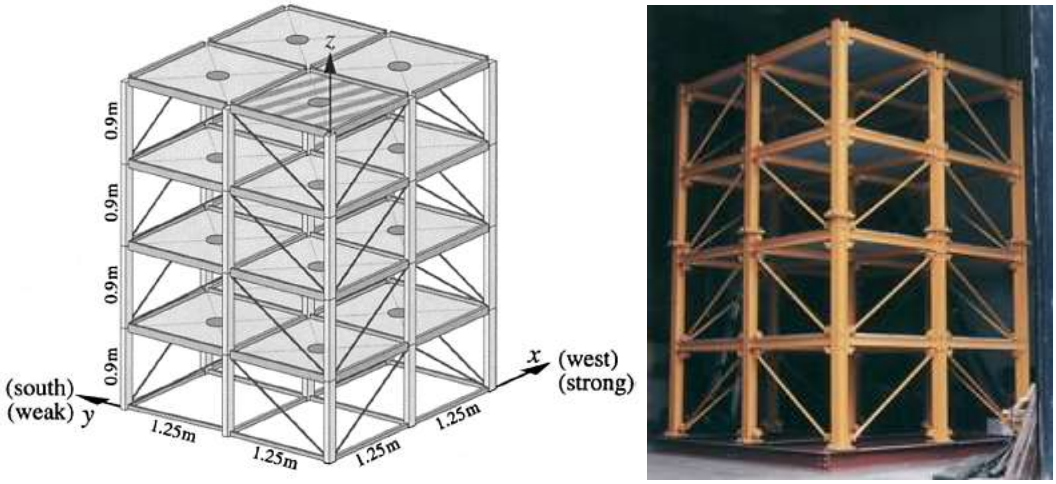

Figure 6 Benchmark Analytical Model (Phase I) and Real Structure (Phase II).

The structure has a 2.5 x 2.5 m base with a height of 3.6 m. The members are made of 300W hot-rolled steel with a nominal yield strength of 300 MPa. The columns are all oriented for greater resistance to bending around the x-axis. The

floor beams are positioned for greater resistance to vertical bending. The braces have no flexural stiffness, so their orientation is irrelevant. There is one slab per bay on each floor, with four 800 kg slabs on the first level, four 600 kg slabs on the second and third levels, and four 400 kg slabs on the fourth floor, or three 400 kg slabs and one 550 kg slab in the case of asymmetric loading.

Two finite element models based on this structure, with 12 and 120 degrees of freedom (DOF), were developed for the generation of simulated data. However, Johnson et al. (2002) recommend using the simpler model (12 DOF) for identification analyses. This is a shear building model with 12 DOF, where the floors (slabs and beams) move as rigid bodies, with translation in x and y and rotation θ around the center of the column, leading to three degrees of freedom per floor. The columns were modeled as Euler-Bernoulli linear elastic beams and the braces as axial bars.

Six damage patterns are considered in the Reference Analytical Phase I and are detailed in Figure 7.

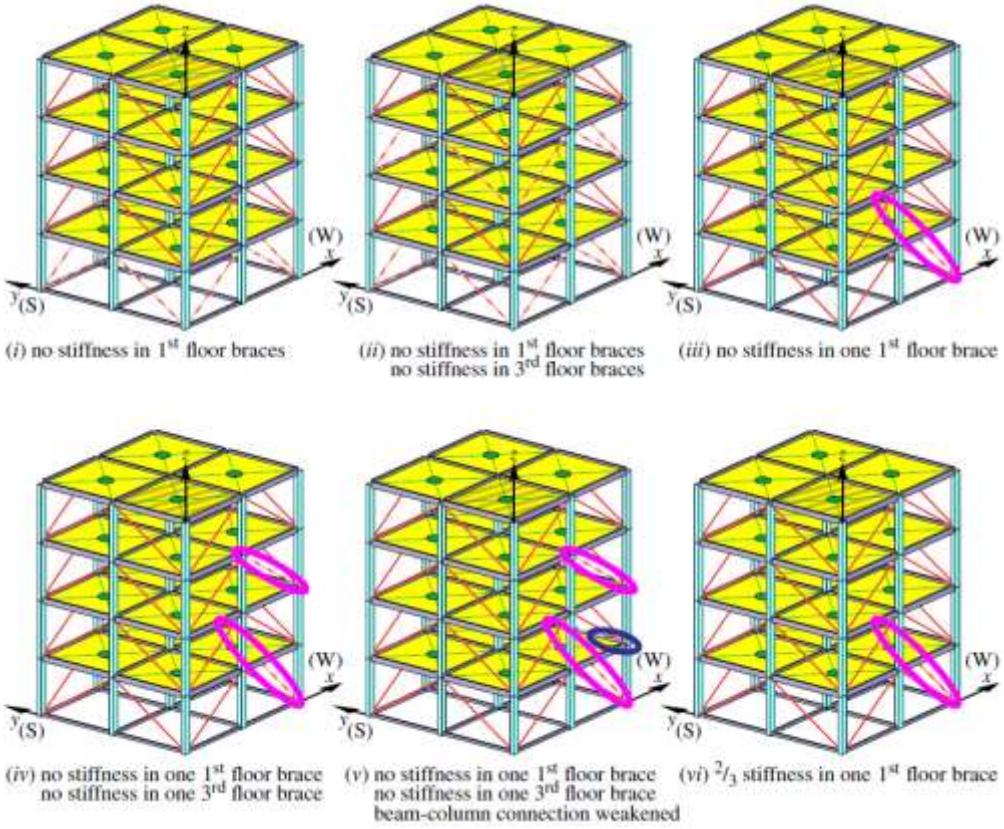

Figure 7 Damage Patterns of Analytical Phase I of the Reference Structure.

Vibration signals were acquired through 16 sensors placed on the structure, four on each floor. Figure 8 shows the positioning of the sensors along the structure and Figure 9 shows an example of a graph of the Benchmark accelerations as a function of the number of observations recorded.

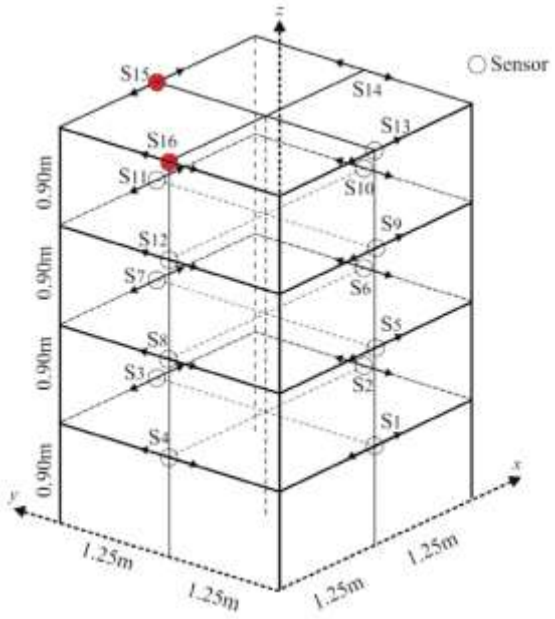

Figure 8 *Location of the sensors.*

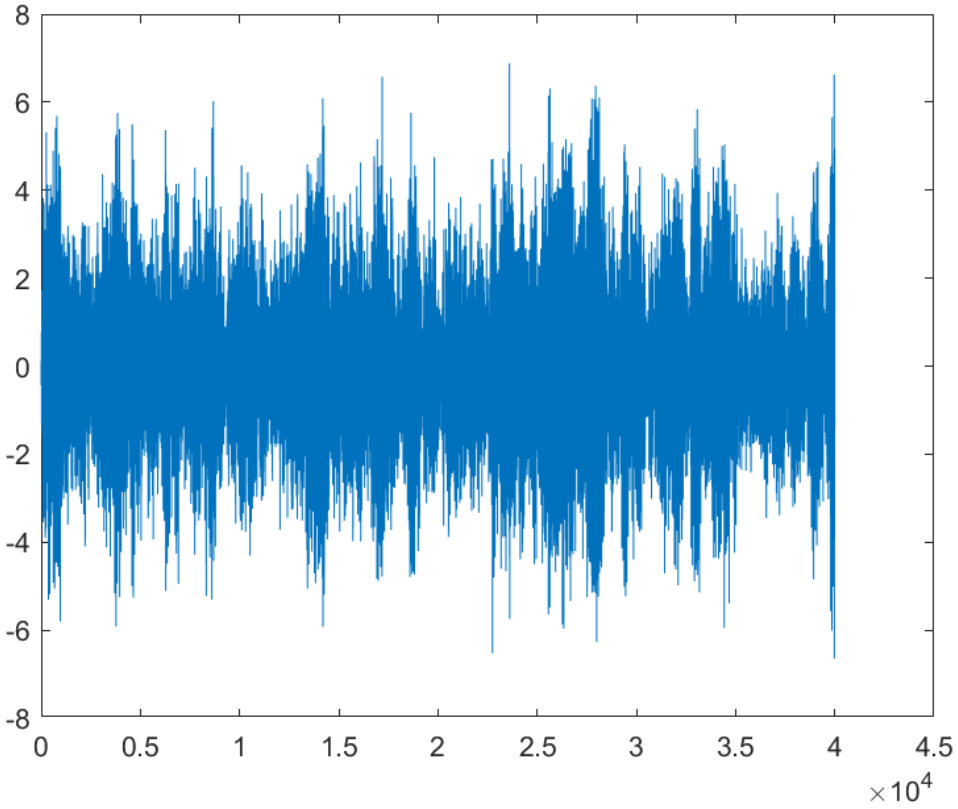

Figure 9 Example of simulated vibration test in FEA for the Benchmark.

Five cases are available in the developed FEA with different considerations regarding the model used, the type of excitation, loading, and other properties. These cases and their considerations are presented in Figure 10.

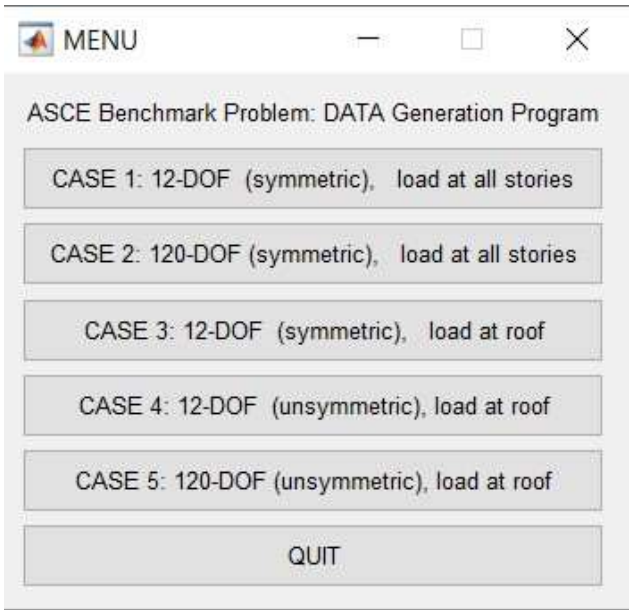

Figure 10 Simulation Case Matrix for the Phase 1 SHM Benchmark Problem.

This paper focuses on the synthetic signals for case 3, which employs a 12-DOF rigid floor model with symmetric mass distribution, excitation due to a diagonal shaker on the roof, four sensors per floor with 10% RMS noise, and unknown input. The structural response is generated based on the parameters adopted by Sanchez et al. (2020) and Sanchez et al. (2022), using a sampling frequency of 1000 Hz over a period of 40 seconds, resulting in 40,000 samples per test. A modal damping ratio of 1% is assigned to each mode. "Seeds" (10, 20, and 30) are used to simulate three different tests for each damage state.

4 METHODOLOGY

An algorithm was developed in Matlab (Mathworks, 2019) to separate the dynamic responses of multiple tests of a structure into structural states according to their damage level. The following describes the methodology used in this research for each damage indicator investigated.

4.1 SDA

The following flowchart (Figure 11) presents the methodology used in the implementation of the SDA damage indicator. The data from the simply supported beam subjected to impact vibration are used as an example.

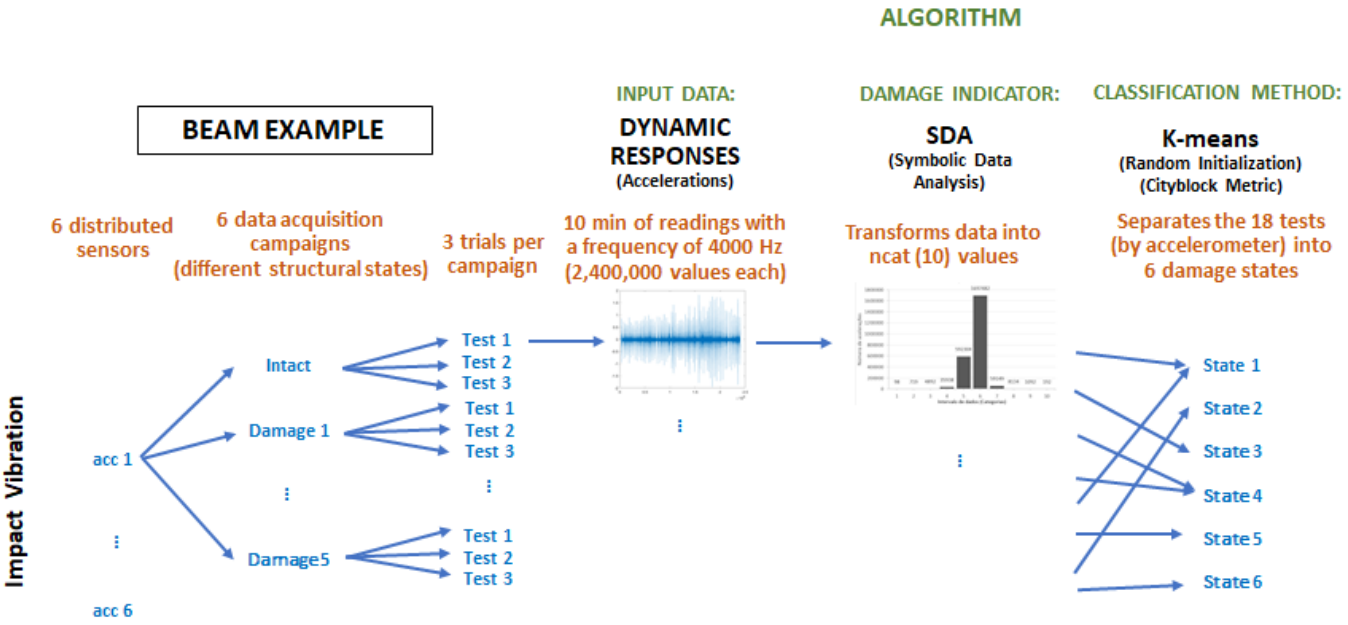

Figure 11 Flowchart of the SDA damage detection algorithm applied to the simply supported beam.

As can be observed, the acceleration histories from the 18 tests (per accelerometer) are transformed into symbolic data and classified by the k-means method according to their similarity using the cityblock metric in 6 structural states. The correct classification of the tests by state represents an indication of a change in the structure.

However, the correct classification of the k-means method depends on an accurate representation of the acceleration data, so that the transformation of the raw data into symbolic data facilitates data manipulation without losing the fundamental characteristics necessary for the classification of the tests by structural state.

For this purpose, two methods for determining the number of categories (intervals) of the SDA were proposed, and the classification results were compared with the results obtained by the representation with 10 categories used by Alves (2016).

This analysis was applied to the accelerations from the simply supported beam, subjected to impact and random vibrations, and from the Benchmark. The results are presented in section 5.1.

4.2 PCA

The following flowchart (Figure 12) presents the methodology used in the implementation of the PCA damage indicator. The data from the Benchmark subjected to random vibration at the top of the structure are used as an example.

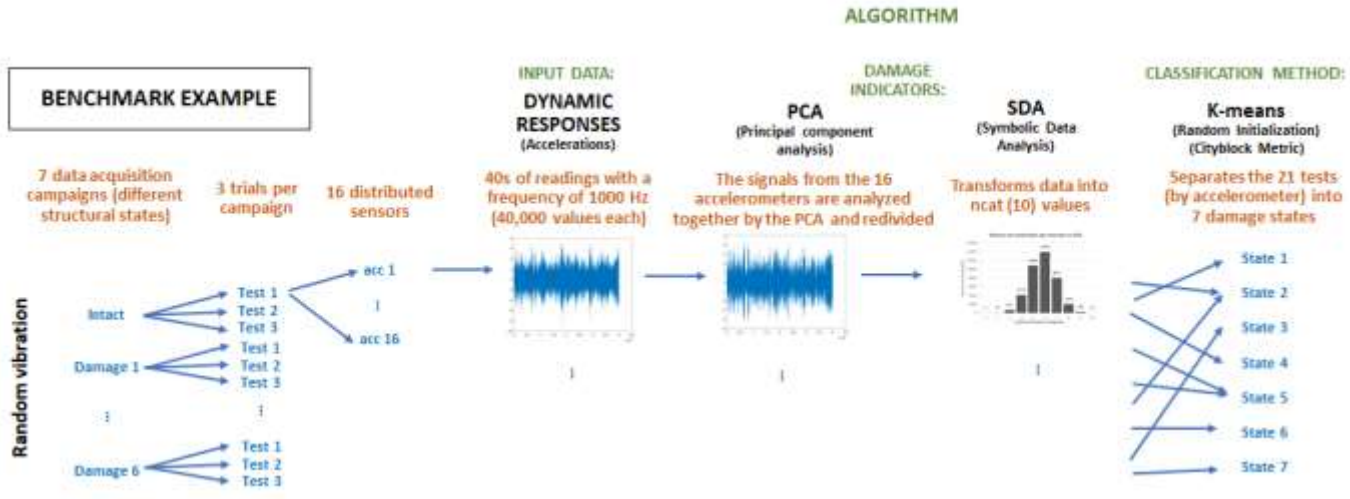

Figure 12 Flowchart of the PCA damage detection algorithm applied to the Benchmark.

As in the previous methodology, the data is transformed into symbolic values, but in this case, the data first undergoes principal component analysis through an orthonormal decomposition to highlight the "main" information.

In this analysis, the number of principal components will be varied, according to the number of accelerometers in each example. The results are presented in section 5.2.

5 RESULTS

5.1 SDA

In Section 2.2, two methods were presented for determining the number of categories used in the SDA: variance analysis with a threshold of 15% (data variance) and Sturges' Rule. Alves (2016) adopts 10 categories in his analyses but does not discuss the motivation behind this choice.

Considering that each test of the simply supported beam has 2.4 million accelerations per accelerometer, the value found for the number of categories using Sturges' Rule (Equation 8) is 22 categories.

For the data variance method, the values diverged depending on the type of excitation and the number of tests used. In the case of random vibration, it was possible to meet the property conservation requirement with 56 categories. For impact vibration, 331 categories were required considering six damage states and 227 when removing the tests from damage level 2 (12 mm hole), referring to the least induced damagedo.

Figures 13 and 14 show the percentages of correct classifications per accelerometer for 6 damage states (a) and 5 damage states (b) considered in the beam, according to the number of categories that describe the data in the SDA, for the cases of random and impact vibration, respectively.

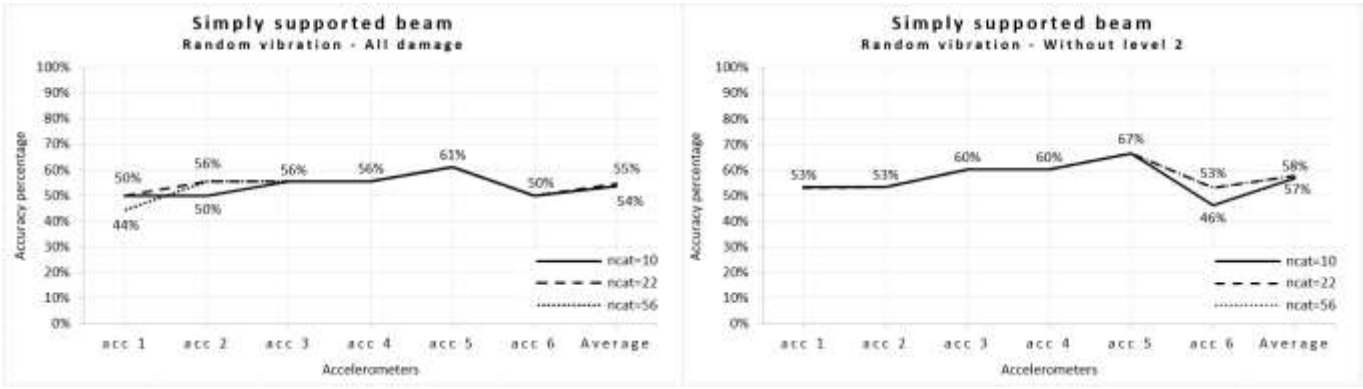

Figure 13: Percentage of correct classifications for six (a) and five (b) damage states of the beam under random vibration.

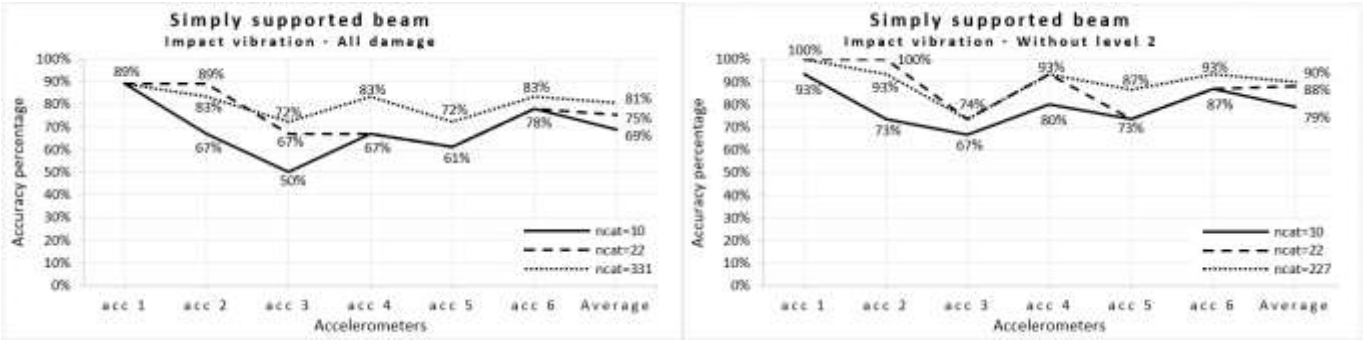

Figure 14: Percentage of correct classifications for six (a) and five (b) damage states of the beam under impact vibration, varying the number of SDA categorie.

It is observed that in the data obtained by random vibration, the change in the number of categories had very little influence on the percentage of correct classifications of the method, with an increase of 1% in the overall average of correct classifications. This demonstrates that in this case, the 10 categories used by Alves (2016) satisfactorily describe the data. Removing the lowest damage state increased the overall average of correct classifications by 3% and the highest average among the accelerometers by 6%.

However, for the data obtained by impact vibration, there was a 12% increase in the overall average of correct classifications, comparing the 10 categories with the value obtained through variance analysis. In the case of the analysis without damage level 2, Sturges' Rule obtained an average 9% higher than the 10 categories and variance analysis 11% higher. Both reaching correct classifications (100% of correct classifications) in the readings of one or two accelerometers.

The increase in the number of categories linearly increases the execution time of the algorithm. In cases with few acceleration values, such as the Benchmark example (40,000 values), this time is in the order of seconds, which does not influence the analysis, but in cases like the beam (2,400,000 values) the analyses with 331 categories reached 3h and 27min (Figure 15).

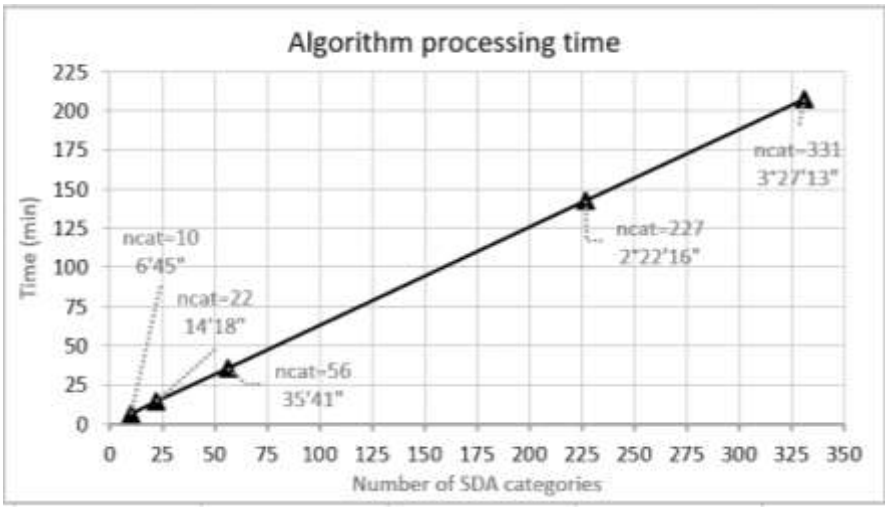

Figure 15: Processing time of the Algorithm (SDA) for the beam data as a function of the number of SDA categories.

Considering the processing time, for cases without initial damage, Sturges' Rule presented advantages over data variance, with an overall average of correct classifications only 2% lower, but a processing time 10 times shorter. Demonstrating that Sturges' Rule presents an acceptable performance with a relatively short processing time and still presenting advantages over the 10 categories (9% more correct classifications).

Figure 16 shows the results for the Benchmark considering 7 damage states (a) and 3 damage states (b), where in the second analysis only the largest damages remained, progressively simulated with the removal of the braces from the 1st and 3rd floors (Figure 7).

Containing 40,000 accelerations per test, Sturges' Rule indicated 16 categories for the Benchmark example. And when the data variance was analyzed, 13 categories were indicated.

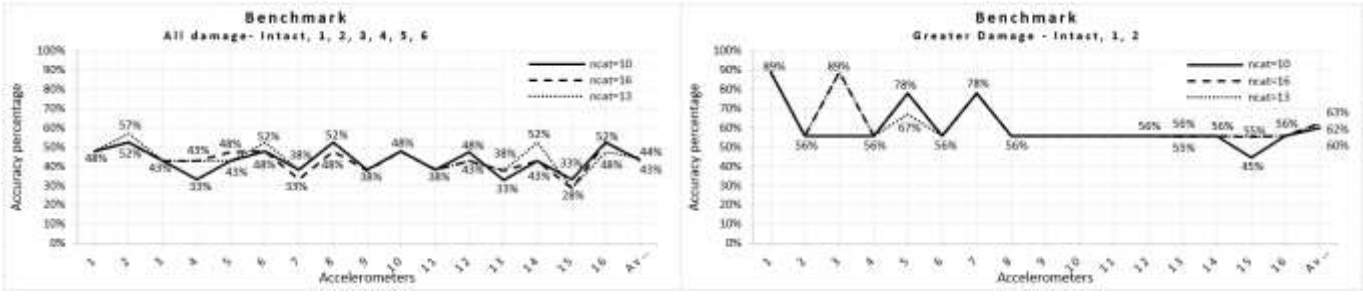

Figure 16: Percentage of correct classifications for seven (a) and three (b) damage states of the Benchmark, varying the number of SDA categories.

For the Benchmark example, the results of the variation of the categories were similar to those of the beam subjected to random vibration. This is due to the fact that the Benchmark is also subjected to a random vibration, which generates signals with lower amplitude and a more uniform representation by the SDA (Figure 17), making it difficult to identify variations in the readings and, consequently, smaller damages end up being hidden.

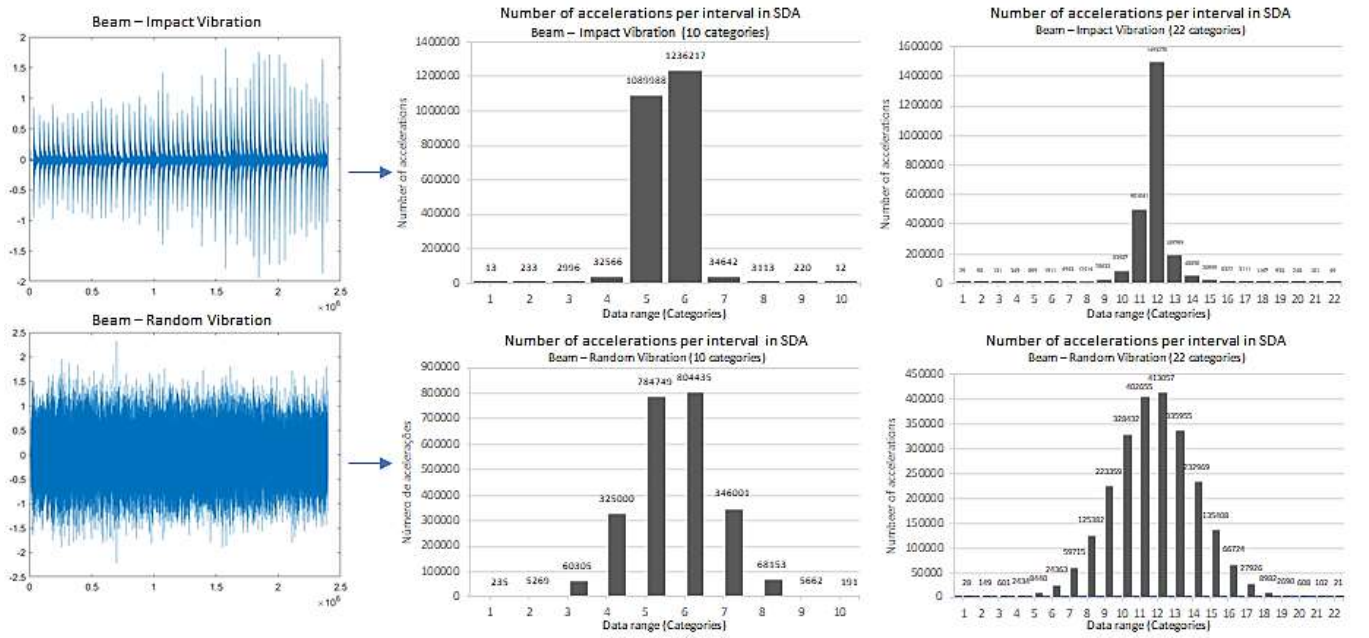

Figure 17: Representation of SDA with 10 and 22 categories for the beam signals under random vibration (top) and impact (bottom).

However, for larger damages and changing the initialization method (sampling to random), it was possible to obtain 100% of correct classifications in the classification of the reading of some accelerometers (Figure 18).

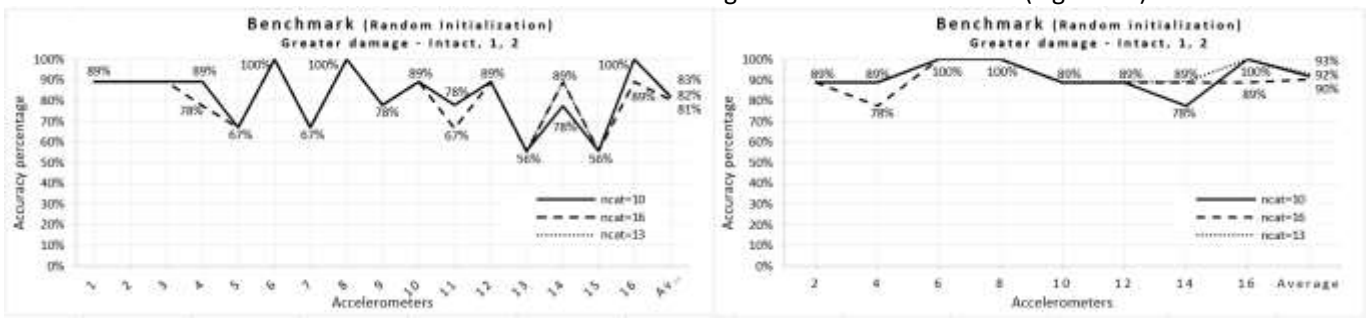

Figure 18: Percentage of correct classifications for three damage states of the Benchmark, with random initialization of centroids, varying the number of SDA categories, with all accelerometers (a) and only pairs (b).

Demonstrating that the verified methods are not sensitive enough to classify damages in their initial phases, but they are quite effective for larger damage levels, especially for signals obtained by impact, obtaining better results according to the choice of ideal parameters for the type of signal read.

It is observed that, in the Benchmark, the even accelerometers (Figure 18a) obtained better results than the odd ones. When analyzed separately (Figure 18b), they raised the overall average of correct classifications by 10%. Probably because they are positioned in the direction of least rigidity of the structure, since the shaker is arranged diagonally and the pillars are positioned for greater resistance to bending around x (Figure 6), allowing greater variations in the acceleration signals due to damages.

Numbers of categories greater than those suggested were tested for both structures, however, there was no significant increase in the percentage of correct classifications.

5.2 PCA

The following (Figures 19 and 20) present the results of the percentages of correct classifications in the classifications as a function of the number of principal components used in the PCA damage indicator. For all analyses, 10 categories were used in the symbolic representation of the data. All principal component values were verified, varying according to the number of accelerometers for each structure (Beam from 1 to 6 and Benchmark from 1 to 16), however, for a better presentation, only the results referring to the principal components that had the highest and lowest

percentage of correct classifications are highlighted, together with the results of 3 principal components, as they were adopted by Alves (2016).

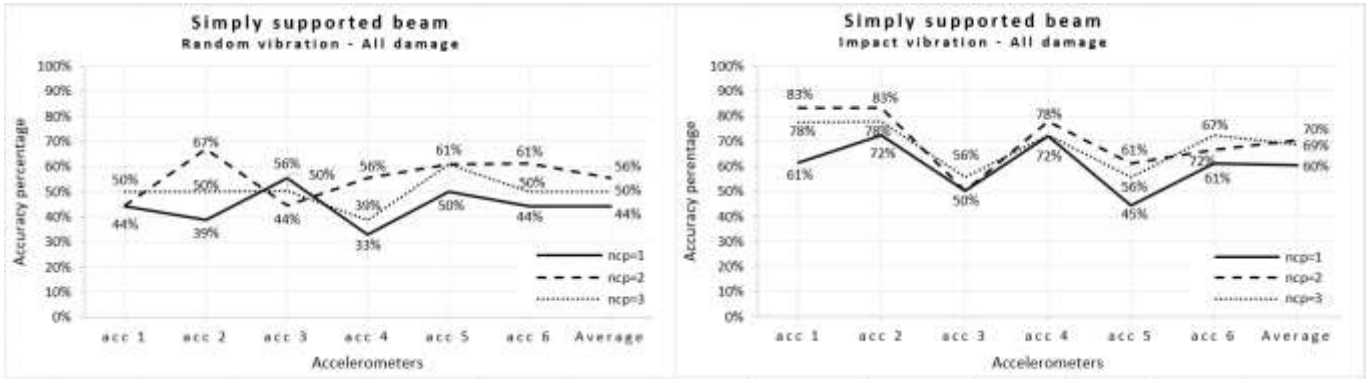

Figure 19: Percentage of correct classifications for the tests of the beam subjected to random vibration (a) and impact vibration (b) using PCA, varying the number of principal components.

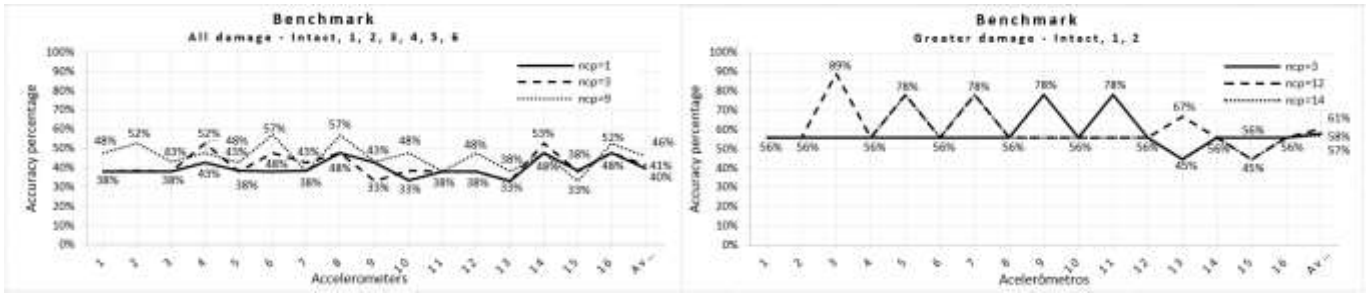

Figure 20: Percentage of correct classifications for the Benchmark tests with seven (a) and three (b) damage states, using PCA, varying the number of principal components.

For the beams, the highest percentage of correct classifications was verified with the adoption of 2 principal components, with an increase of 6% in the average of correct classifications for the case of random vibration and 1% for impact, compared to the 3 principal components. However, for the Benchmark, the value diverged depending on the number of damage states verified. Considering the 7 damage states, with 9 principal components there was a 5% increase in the percentage of correct classifications, and, with 3 states, the indicated value was 14 principal components, increasing the overall average of correct classifications by 3%, compared to 3 components.

It is noted that the increases were not significant. Therefore, a prior study of the number of principal components for each structure would not be justified.

5 CONCLUSION

Damage classification with indicators such as SDA and PCA is more effective using impact vibration data, as they have higher amplitude, and their differences are better represented by symbolic data than data obtained by random vibration.

Among the suggested techniques for determining the number of SDA categories, the one that presented the best results, considering the percentage of correct classifications in the classification of damage states and the processing time of the algorithm, was Sturges' Rule. Both for short and long signals, obtained by random vibration or by impact. Proving to be an appropriate method to solve the problem of determining the number of intervals.

The variation of the number of principal components did not present significant increases in the percentages of correct classifications using PCA. Demonstrating that adopting an average value for the number of principal components is a practical and efficient approach, thus not justifying a prior study of the number of components for each type of structure.

6 ACKNOWLEDGMENTS

The authors gratefully acknowledge the financial support of CNPq (Brazil), which made this research possible.

Author's Contribuitions: Conceptualization, R Vasconcelos, G Doz and JLV Brito; Methodology, R Vasconcelos; Investigation, R Vasconcelos; Writing - original draft, R Vasconcelos; Writing - review & editing, R Vasconcelos, G Doz and JLV Brito; Funding acquisition, JLV Brito; Resources, JLV Brito; Supervision, G Doz and JLV Brito.

Editor: Marco L. Bittencourt

References

Abdeljaber, O.; Avci, O.; Kiranyaz, S.; Gabbouj, M.; Inman, D. J. (2017). Real-time vibration-based structural damage detection using one-dimensional convolutional neural networks. Journal of Sound and Vibration, v. 388, p. 154-170.

Alves, V.N. (2012). Study of new strategies for identifying structural damage from vibrational data. MSc. Dissertation (in Portuguese), Federal University of Ouro Preto, Brazil.

Alves, V.N. (2016). Abnormality techniques applied to structural damage detection. Ph.D. Thesis (in Portuguese), Federal University of Ouro Preto, Brazil.

Alves, V.; Cury, A.; Roitman, N.; Magluta, C.; Cremona, C. (2015). Novelty detection for SHM using raw acceleration measurements. Structural Control and Health Monitoring, 22(9), 1193–1207, doi:10.1002/stc.1741.

Amaral, R.P.F. (2022). Artificial intelligence applied to structure monitoring: Detection of mechanical-structural changes based on the use of sparse autocoding neural networks to characterize dynamic responses. Ph. D. Thesis (in Portuguese), Federal University of Juiz de Fora, Brazil.

Avci, O.; Abdeljaber, O.; Kiranyaz, S.; Hussein, M.; Gabbouj, M.; Inman, D. J. (2021). A review of vibration-based damage detection in civil structures: From traditional methods to Machine Learning and Deep Learning applications. Mechanical Systems and Signal Processing, 147, 107077. doi: 10.1016/j.ymssp.2020.107077.

Bang, S.; Park, S.; Kim, H.; Kim, H. (2019). Encoder-decoder network for pixel-level road crack detection in black-box images. Comput.-Aided Civ. Infrastruct. Eng., 34(8): 713-727.

Bel-Hadj, Y.; Fernandes, A.; Weijtjens W.; Devriendt, C. (2024) Feasibility study on monitoring the structural health of a transmission tower with controlled damage scenarios. Journal of Physics: Conference Series, v. 2647, doi: 10.1088/1742-6596/2647/18/182037.

Bourdalos, D.M., Zisopoulos, S.S.; Tcherniak, D.; Sakellariou, J. S. (2024) An experimental study on the performance of virtual sensing using optimal and regular physical sensors placement. Journal of Physics: Conference Series, v. 2647, doi: 10.1088/1742-6596/2647/19/192003.

Branco, H. (2013). Bridge collapses: Lessons learned. (in Portuguese), Higher Institute of Engineering in Lisbon, Portugal.

Bru, D.; Ivorra, S.; Torres, B. (2024) Dynamic changes on a masonry cross vault after a forced damage. Journal of Physics: Conference Series, v. 2647, doi: 10.1088/1742-6596/2647/18/182011.

Cardoso, R.A.; Cury, A.; Barbosa, F. (2019a). Automated real-time damage detection strategy using raw dynamic measurements. Engineering Structures, 196, 109364. DOI: 10.1016/j.engstruct.2019.109364.

Cardoso, R.A.; Cury, A.; Barbosa, F.; Gentile, C. (2019b). Unsupervised real-time SHM technique based on novelty indexes. Structural Control and Health Monitoring, e2364. DOI: 10.1002/stc.2364.

Chaim, L.P.; Chavarette, F.R.; Lopes, M.L.M. (2018). Characterization of Fault Patterns across a Network Artificial Neural Fuzzy ARTMAP. (in Portuguese). Proceeding Series of the Brazilian Society of Applied and Computational Mathematics, v. 6, n. 1.

Chen, S.X.; Zhou, L.; Ni, Y.; Liu, X. (2021). An acoustic-homologous transfer learning approach for acoustic emission–based rail condition evaluation. Struct. Health Monit., 20(4): 2161-2181, doi: 10.1177/1475921720976941.

Crémona, C.; Cury, A.; Orcesi, A.; Dieleman, L. (2011). Symbolic data analysis and supervised/non supervised learning algorithms for bridge health monitoring. In. 9th World Congress on Railway Research, 9., 2011. Lille. Anais... Lille: World Congress on Railway Research.

Cury, A. (2010). Abnormality techniques applied to structural health monitoring. Ph.D. Thesis (in French), Paris-Est University, France.

Cury, A.A.; Crémona, C.; Diday, E. (2010). Application of symbolic data analysis for structural modification assessment. Enginnering Structures, v. 32, n. 3, p. 762-775, DOI: 10.1016/j.engstruct.2009.12.004.

Cury, A.A.; Crémona, C. (2012). Assignment of structural behaviours in long-term monitoring: application to a strengthened railway bridge. Structural Health Monitoring, v. 11, n. 4, p. 422-441, DOI: 10.1177/1475921711434858.

Cury, A.A.; Crémona, C.; Dumoulin, J. (2012). Long-term monitoring of a PSC box girder bridge: operational modal analysis, data normalization and structural modification assessment. Mechanical Systems and Signal Processing, v. 33, p. 13-37, DOI: 10.1016/j.ymssp.2012.07.005.

Cury, A.A.; Ribeiro, D.R.F.; Melo, A.D. (2014). Structure Monitoring Techniques: A Comprehensive Review. (in Portuguese), 1. ed. São Paulo: Text Workshop, p. 248.

Dackermann, U.; Smith, W.A.; Randall, R.B. (2014). Damage identification based on response-only measurements using cepstrum analysis and artificial neural networks. Structural Health Monitoring, v. 13, n. 4, p. 430-444.

Dackermann, U.; Smith, W.A.; Alamdari, M.M.; Li, J.; Randall, R. B. (2018). Cepstrum-based damage identification in structures with progressive damage. Structural Health Monitoring, v. 18, n. 1, p. 87-102.

Dederichs A.C..; Øiseth, O. (2024) A new fully automated operational modal analysis algorithm intended for large civil structures. Journal of Physics: Conference Series, v. 2647, doi: 10.1088/1742-6596/2647/19/192009.

Delo, G.; Mattone, M.; Surace, C.; Worden, K. (2024) Novelty detection across a small population of real structures: A negative selection approach. Journal of Physics: Conference Series, v. 2647, doi: 10.1088/1742-6596/2647/19/192004.

Doebling, S. W.; Farrar, C. R.; Prime, M. B. (1998). A Summary Review of Vibration- Based Damage Identification Methods. The Shock and Vibration Digest.

Drangsfeldt, C.A.; Avendaño-Valencia, L.D. (2024). A combined implicit-explicit vibration-based SHM method for damage detection of wind turbine blades. Journal of Physics: Conference Series, v. 2647, doi: 10.1088/1742-6596/2647/18/182030.

Duan, Y.; Chen, Q.; Zhang, H.; Yun, C. B.; Wu, S.; Zhu, Q. (2019). CNN-based damage identification method of tied-arch bridge using spatial-spectral information. Smart Struct. Syst, 23(5): 507-520, doi: https://doi.org/10.12989/sss.2019.23.5.507.

Fan, X.; Li, J.; Hao, H. (2021). Review of piezoelectric impedance based structural health monitoring: Physics-based and data-driven methods. Adv. Struct. Eng., 24(16): 3609-3626, doi: 10.1177/13694332211038444.

Farrar, C.R., Worden, K. (1975). An Introduction to Structural Health Monitoring, Springer, p. 1-7.

Farrar, C.R., Worden, K. (2012). Structural Health Monitoring: A Machine Learning Perspective. Chichester.

Fontana, A.; Naldi, M. C. (2009). Comparison Study of Methods for Estimating Group Numbers in Data Grouping Problems. (in Portuguese), São Carlos: ICMC.

Friswell, M. I. (2007). Damage identification using inverse methods. Philosophical transactions. Series A, Mathematical, physical, and engineering sciences, v. 365, n. 1851, p. 393–410.

Hastie, T.; Tibshirani, R.; Friedman, J. (2009). The Elements of Statistical Learning: Data Mining, Inference, and Prediction. 2. ed. Stanford: Springer.

Haykin, S. (2008). Neural networks and learning machines. Pearson, ed. 3, ISBN-13: 978-0-13-147139-9.

Hickman, G.A.; Gerardi, J. J.; Feng, Y. (1991) Application of Smart Structures to Aircraft Health Monitoring. Journal of Intelligent Material Systems and Structures, 2(3), p. 411–430, Doi:10.1177/1045389x9100200308.

Jesus, W.P.; Lima, E.J.G.; Alvares, R.G.; Silva, J.R.; Rocha, D.A.; Peixoto, Z.M.A. (2020). Application of machine learning techniques for vibration monitoring and crack detection in bridges. (in Portuguese), Proceedings of the Brazilian Automatic Congress, ISSN 2525-8311, v. 2, n. 1, doi: https://doi.org/10.48011/asba.v2i1.1269.

Johnson, E.A.; Lam, H.F.; Katafygiotis, L.S.; Beck, J.L. (2002). The Phase I IASC-ASCE Structural Health Monitoring Benchmark Problem using Simulated Data. Journal of Engineering Mechanics.

Kullaa, J. (2024) Damage detection using different types of sensors. Journal of Physics: Conference Series, v. 2647, doi: 0.1088/1742-6596/2647/18/182006.

Latha, L.; Ray-Chaudhuri, S. (2024). Damage Identification in Masonry Wall Specimens: Shake Table Studies. Journal of Physics: Conference Series, v. 2647, doi: 10.1088/1742-6596/2647/19/192022.

Lu, H.; Mardanshahi, A.; Cantero-Chinchilla, S.; Gryllias, K.; Chronopoulos, D. (2024). Uncertainty quantification of damage localization based on a probabilistic convolutional neural network. Journal of Physics: Conference Series, v. 2647, doi: 10.1088/1742-6596/2647/18/182022.

Masmeijer, T.C.P.; Méndez Echenagucia, T.; Slavič, J.; Loendersloot, R.; Habtour, E. (2024). Effect of eccentricity on sensing in spider web inspired cable nets. Journal of Physics: Conference Series, v. 2647, doi: 10.1088/1742-6596/2647/19/192012.

Mathworks. (2019). MATLAB R 2019b. v.9.7.0.

Mazzeo, M.; De Domenico, D.; Quaranta, G.; Santoro, R. (2024) Modal Parameters identification in existing bridges based on free vibration tests. Journal of Physics: Conference Series, v. 2647, doi: 10.1088/1742-6596/2647/18/182026.

Nozari A., Behmanech I., Yousefianmoghadam S., Moaveni B., Stavridis A. (2017). Effects of variability in ambient vibration data on model updating and damage identification of a 10-story building. Engineering Structures, v. 151, p. 540-53.

Pandey, A.K.; Biswas, M. (1994). Damage Detection in Structures Using Changes in Flexibility. Journal of Sound and Vibration, v.169, n. 1, p. 3-17.

Pimentel, E.P.; França, V.F.; Omar, N. (2003). The identification of groups of learners in face-to-face teaching using clustering techniques. (in Portuguese), Proceedings of the Brazilian Symposium on Informatics in Education, v. 1, n. 1, p. 495–504.

Rashid, D.S.; Giorgio-Serchi, F.; Hosoya N.; Garcia Cava, D. (2024). Estimation of bolt tension using transverse natural frequencies of the shank and protruding end. Journal of Physics: Conference Series, v. 2647, doi: 10.1088/1742-6596/2647/18/182005.

Ren, W. -X.; Peng, X. -L. (2005). Baseline finite element modeling of a large span cable-stayed bridge through field ambient vibration tests. Computers and Structures, v. 83, p. 536-50.

Rojas, C.J.G.; Bittencourt, M.L.; Boldrini, J.L. (2019). Solution and oarameter identification of a damage model using a deep learning approach. Proceedings of the XL Ibero-Latin-American Congress on Computational Methods in Engineering, ABMEC, Brazil.

Rytter, T. (1993). Vibration based inspection of civil engineering structure. Aalborg University.

Sabbà, M.F.; Rizzo, F.; Giannoccaro, N.I.; Mansour, S.; La Scala, A.; Foti, D. (2024). Characterization and dynamic behaviour of Masonry Newly Concept Vault realized by 3d Printer. Journal of Physics: Conference Series, v. 2647, doi: 10.1088/1742-6596/2647/19/192016.

Sanayei, M.; Khaloo, A.; Gul, M.; Catbas, F.N. (2015). Automated finite element model updating of a scale bridge model using measured static and modal test data. Engineering Structures, v. 102, p. 66-79.

Sanchez, W.D.; Brito, J.V.; Avila, S.M. (2020). Structural Health Monitoring Using Synchrosqueezed Wavelet Transform on IASC-ASCE Benchmark Phase I. International Journal of Structural Stability and Dynamics, vol. 20, n. 12, p. 14, DOI: 10.1142/s0219455420501382.

Sanchez, W.D.; Avila, S.M.; Brito, J.V. (2022). A methodology based on empirical mode decomposition and synchrosqueezed wavelet transform for modal properties identification and damage detection. Journal of the Brazilian Society of Mechanical Sciences and Engineering, DOI: 10.1007/s40430-022-03818-y.

Soares, D.A.C. (2022). Development of a system for automatic monitoring of structural integrity. MSc. Dissertation (in Portuguese), Federal University of Juiz de Fora, Brazil.

Sony, S., Gamage, S.; Sadhu, A.; Samarabandu, J. (2022). Vibration-based multiclass damage detection and localization using long short-term memory networks. Structures. 35: 436-451, doi: https://doi.org/10.1016/j.istruc.2021.10.088.

Sturges, H.A. (1926). The choice of a class interval. Journal of the American Statistical Association, 21(153), 65-66.

Teng, S.; Chen, G.; Liu, G.; Lv, J.; Cui, F. (2019). Modal Strain Energy-Based Structural Damage Detection Using Convolutional Neural Networks. Applied Sciences, 9, 3376, doi: 10.3390/app9163376.

Tomassini, E.; García-Macías, E.; Reynders, E.; Ubertini, F. (2024) Modal analysis for damage identification of partially continuous multi-span bridges. Journal of Physics: Conference Series, v. 2647, doi: 10.1088/1742-6596/2647/19/192006.

Vadyala, S.R.; Betgeri, S.N.; Matthews, J.C.; Matthews, E. (2022). A review of physics-based machine learning in civil engineering. Results Eng., 13: 100316, doi: https://doi.org/10.1016/j.rineng.2021.100316.

Wang, Y.W.; Ni, Y.Q. (2020). Bayesian dynamic forecasting of structural strain response using structural health monitoring data. Struct. Control Health Monit., 27(8): 2575, doi: 10.1002/stc.2575.

Weijtjens, W.; Oliveira Junior, A.F.; Cloet, B.; Yilmaz, Ö.C.; Devriendt C. (2024) Large scale test of vibration based icing detection for wind turbines. Journal of Physics: Conference Series, v. 2647, doi: 10.1088/1742-6596/2647/19/192008.

Wojtczak, E.;Rucka, M.; Andrzejewska, A. (2024) Damage detection in 3D printed plates using ultrasonic wave propagation supported with weighted root mean square calculation and wavefield curvature imaging. Journal of Physics: Conference Series, v. 2647, doi: 10.1088/1742-6596/2647/18/182003.

Yuvaraj, N.; Kim, B.; Preethaa, K.R.S. (2020). Transfer learning based real-time crack detection using unmanned aerial system. Int. J. High-Rise Build., 9(4): 351-360, doi: https://doi.org/10.21022/IJHRB.2020.9.4.351.

Yuan, L.; Ni, Y.; Rui, E.; Zhang, W. (2024). Structural damage inverse detection from noisy vibration measurement with physics-informed neural networks. Journal of Physics: Conference Series, v. 2647, doi: 10.1088/1742-6596/2647/19/192013.

Zhang, Q.H.; Ni, Y.Q. (2022). A bayesian hypothesis testing-based statistical decision philosophy for structural damage detection. *Struct. Health Monit.*: 14759217221133292, doi: 10.1177/14759217221133292.